Investigation of Wide-FSR SOI Optical Filters Operating in C and L Bands

Benedetto Troia, Vittorio M. N. Passaro, *Senior Member, IEEE*, and Francesco De Leonardis

***Abstract* — In this paper we present the investigation of optical filters based on triple ring resonator architectures in silicon-on-insulator technology. The generalized approach based on Mason's rule and delay line signal processing has been implemented for modeling optical filters in Z-domain. A numerical investigation based on the coefficient map has been adopted for designing optical add-drop multiplexers with wide free spectral ranges, as large as 12 THz (~ 96 nm). Low crosstalk, of the order of -20 dB, has been numerically demonstrated in overall transmittances of optimized filters.**

***Keywords* — Free spectral range, optical add-drop multiplexers, ring resonators, silicon-on-insulator.**

I. Introduction

NOWADAYS optical networks represent the backbone of telecommunication systems, characterized by wide bandwidths and ultra-high data rates, up to 320 Gb/s [1].

Optical networks based on dense wavelength division multiplexing (DWDM) technology are developed to support a huge bandwidth increase [2]. Conventional DWDM systems are characterized by a high wavelength density (i.e., 160 wavelengths), with 25 GHz spacing (i.e., 0.2 nm @1.55 μm) or better. In this context, advanced optical filters represent an important network element. Photonic architectures based on single or multiple ring resonators (RR) have been widely used as tunable optical filters [3], optical add-drop multiplexers (OADM) [4], reconfigurable-OADMs [5]-[7], optical de-multiplexers and routers [4], to name a few.

In particular, OADMs operating in C and L bands (1520-1630 nm) are generally characterized by a wide bandwidth, high extinction ratio, low crosstalk and free spectral range (FSR), typically ranging from hundreds of GHz to a maximum of a few THz (e.g., ~ 2 THz or 17 nm). The main drawback of using RRs is represented by their large number of resonances and FSRs of a few of nanometers, limiting the application of OADMs when a unique resonance has to be filtered (i.e., add or drop) over a relatively large bandwidth (e.g., 30 nm for C-band). Moreover, the typical approach used for expanding FSR in RR architectures consists in reducing the radius R, as reported in [8]. In particular, a 1.5 μm-radius RR has been designed with FSR = 52 nm (6.35 THz). However, radiation losses tend to exponentially increase with reduction of RR radius, limiting its length to a minimum of about 3 μm.

To this purpose, different solutions for expanding FSRs in integrated OADMs have been presented in literature. In particular, a novel architecture with both RRs and photonic bandgap structures has been investigated, exhibiting a FSR larger than 140 nm [9]. A multiple photonic crystal RR architecture has been proposed for overcoming the problem of radiation losses induced by small radii of conventional RRs based on silicon-on-insulator (SOI) waveguides (e.g., strip, rib) [10]. Recently, a single ring interferometer configuration has been experimentally demonstrated [11]. It produces a doubled FSR by in-phase combining light from pass-through port and drop port of the resonator. In conclusion, multiple RR architectures have been proposed, such as an optical channel dropping filter in GaInAsP-InP with FSR = 40 nm [12]. A vertically triple coupled RR filter based on the Vernier effect and characterized by FSR = 25.8 nm has been also designed [13]. Both these configurations require high fabrication accuracy and are not suitable for mass scale production.

In this paper we present the investigation of optical filters based on triple RR architectures, operating in C and L bands and CMOS-compatible, thus suitable for mass scale production and integration. Proposed filters are based on standard SOI rib waveguides designed at 1.55 μm and simulated by full-vectorial 2D Finite Element Method (FEM) [14].

A numerical analysis based on the coefficient map has been implemented for designing optical filters with a desired FSR. In addition, interesting properties have been numerically demonstrated. In fact, wide FSRs larger than 10 THz have been achieved with more relaxed sizes, i.e., radii larger than 5 μm, so preventing high radiation losses which can degrade the device performance. Crosstalk as low as -16.5 dB has been evaluated for an optical filter designed with FSR = 12 THz.

II. Modeling of Optical Filters

The modeling of optical filters based on a triple RR architecture consists in the implementation of the generalized approach based on Mason's rule and delay line signal processing in Z-transform domain [15]. In particular, it is possible to define in a single RR the single

This work has been partially supported by Fondazione della Cassa di Risparmio di Puglia, Bari, Italy.

B. Troia is with Photonics Research Group, Dipartimento di Elettrotecnica ed Elettronica, Politecnico di Bari, Via Edoardo Orabona n. 4, 70125 Bari – Italy, (e-mail: ing.b.troja@gmail.com).

V. M. N. Passaro is head of Photonics Research Group, Dipartimento di Elettrotecnica ed Elettronica, Politecnico di Bari, Via Edoardo Orabona n. 4, 70125 Bari – Italy, (phone: +39 0805963850; e-mail: passaro@deemail.poliba.it).

F. De Leonardis, is with the Photonics Research Group, Dipartimento di Elettrotecnica ed Elettronica, Politecnico di Bari, Via E. Orabona n. 4, 70125 Bari – Italy, (e-mail: f.deleonardis@poliba.it).

roundtrip delay T_i, as follows:

$$T_i = \frac{L_i \cdot n_{eff,i}}{c} \quad (1)$$

where L_i is the single roundtrip length of the i^{th} RR (i.e., RR perimeter), c is the light velocity in vacuum and $n_{eff,i}$ is the effective index of the optical mode propagating in i^{th} RR. A SOI rib waveguide has been selected for input and output buses and RRs, designed at wavelength λ_{op} = 1.55 μm. The optical field spatial distribution and the corresponding effective index have been calculated by full-vectorial FEM, using at least 67,000 triangular vector-elements and a domain region with a total area of 16 μm^2 (4 μm × 4 μm). Simulation of quasi-TE polarized optical E-field is plotted in Fig. 1.

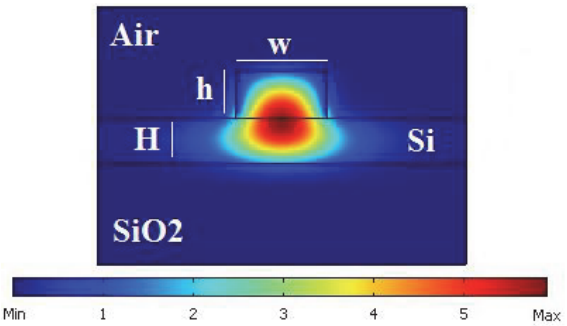

Fig. 1. Ex-field (quasi-TE) spatial distribution in the SOI rib waveguide with w = 1 μm, h = 500 nm, H = 500 nm.

Effective indices calculated for quasi-TE and quasi-TM polarized optical fields are $n_{eff,TE}$ = 3.323135 and $n_{eff,TM}$ = 3.308568, respectively. However, quasi-TE polarization is selected for design purposes, since it ensures a stronger optical field confinement over quasi-TM.

Once defined the single roundtrip delay T in a RR, it is possible to introduce the FSR expression as follows:

$$FSR_i = \frac{1}{T_i} = \frac{c}{L_i \cdot n_{eff,i}} \quad (2)$$

By observing Eq. (2), the smaller the ring circumference, the larger the FSR, according to the design solution adopted in Ref. [8].

The delay line signal processing allows realizing the triple RR optical filter schematic in Z-transform domain, properly named a signal flow graph (SFG), as sketched in Fig. 2(b). Assuming the optical filter as linear and time invariant, each RR can be represented in a cascaded configuration with delay blocks characterized by different coefficients M, N and O, being natural and co-prime numbers. In this way, each delay accumulated by the optical signal propagating in a single RR of the cascaded architecture, is an integer multiple of the unit delay T, previously defined in Eq. (1). Moreover, coefficients M, N and O take into account the different perimeter lengths L_i of RRs constituting the cascaded architecture.

Directional couplers in Fig. 2(a) with power coupling ratios k_1, k_2, k_3 and k_4 are schematized in SFG by coefficients C_i and S_i, representing through and cross port transmission of the i^{th} coupler, respectively, as:

$$C_i = \sqrt{1-k_i}\,, \quad -jS_i = -j\sqrt{k_i} \quad (3)$$

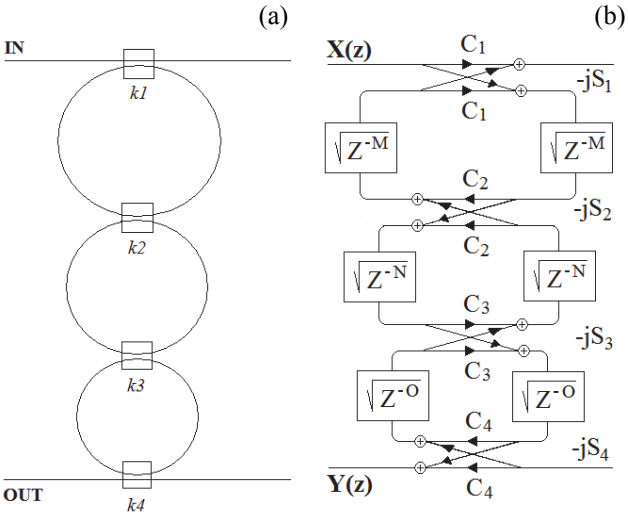

Fig. 2. (a) Schematic of triple ring resonator architecture and (b) its corresponding signal flow graph (SFG) in Z-transform domain.

Mason's rule has been used to calculate the overall transmittance of the triple RR architecture proposed in this paper. To this purpose, a brief explanation of the method applicable to a general system architecture is presented below. The overall transmittance is given by:

$$T_f(z) = \frac{Y(z)}{X(z)} = \frac{\sum_{k=1}^{P} T_k(z)\Delta_k}{\Delta}, \text{ with}$$
$$\Delta = 1 - \sum_i T_i(z) + \sum_{ij} T_i(z)T_j(z) + \quad (4)$$
$$- \sum_{ijn} T_i(z)T_j(z)T_n(z) + \ldots + (-1)^m \sum \ldots + \ldots$$

whose parameters are listed as follows:

- P = total number of forward paths between $X(z)$ and $Y(z)$;
- $z = \exp(j2\pi Tv)$, v being the optical frequency;
- $T_f(z)$ is the overall transmittance of any SFG;
- $X(z)$ is the input variable in Z-domain;
- $Y(z)$ is the output variable in Z-domain;
- $T_k(z)$ is the transmittance of k^{th} forward path;
- Δ is the determinant of the graph;
- $T_i(z)$ is the transmittance of SFG i^{th} individual loop;
- $T_i(z)T_j(z)$ is the product of transmittances of all possible combinations of two non-touching loops;
- $T_i(z)T_j(z)T_n(z)$ is the product of transmittances of all possible combinations of three generic non-touching loops;
- Δ_k is the cofactor value of Δ for the k^{th} forward path, after removing the loops touching the k^{th} forward path.
- $\gamma_i = \exp(-\alpha L_i)$, is the roundtrip loss of i^{th} RR with perimeter length L_i and average ring loss per unit length α_i.
- q_i is the amplitude transmission coefficient of the i^{th} coupler.

A validation procedure using all numerical data from Ref. [15] has been carried out, before applying our

generalization [16]. Referring to SFG as shown in Fig. 2(b), the number of forward paths P from $X(z)$ to $Y(z)$ can be set to one. In addition, the transmittance of the single forward path is written as follows:

$$T_1(z)\Delta_1 = q_1 q_2 q_3 q_4 S_1 S_2 S_3 S_4 \sqrt{z^{-(M+N+O)}\gamma_1\gamma_2\gamma_3} \quad (5)$$

Consequently, the transmittances of all individual loops have been calculated as:

$$T_1^3(z) = q_1 q_2 C_1 C_2 \gamma_1 z^{-M} \quad (6.a)$$

$$T_2^3(z) = q_2 q_3 C_2 C_3 \gamma_2 z^{-N} \quad (6.b)$$

$$T_3^3(z) = q_3 q_4 C_3 C_4 \gamma_3 z^{-O} \quad (6.c)$$

$$T_4^3(z) = -q_1 q_2^2 q_3 C_1 C_3 S_2^2 \gamma_1\gamma_2 z^{-(M+N)} \quad (6.d)$$

$$T_5^3(z) = -q_2 q_3^2 q_4 C_2 C_4 S_3^2 \gamma_2\gamma_3 z^{-(N+O)} \quad (6.e)$$

$$T_6^3(z) = q_1 q_2^2 q_3^2 q_4 C_1 C_4 S_2^2 S_3^2 \gamma_1\gamma_2\gamma_3 z^{-(M+N+O)} \quad (6.f)$$

The products of transmittances of all possible combinations of two and three non-touching loops are listed below:

$$T_{1,2}^3(z) = q_1 q_2^2 q_3 C_1 C_2^2 C_3 \gamma_1\gamma_2 z^{-(M+N)} \quad (7.a)$$

$$T_{1,3}^3(z) = q_1 q_2 q_3 q_4 C_1 C_2 C_3 C_4 \gamma_1\gamma_3 z^{-(M+O)} \quad (7.b)$$

$$T_{2,3}^3(z) = q_2 q_3^2 q_4 C_2 C_3^2 C_4 \gamma_2\gamma_3 z^{-(N+O)} \quad (7.c)$$

$$T_{4,3}^3(z) = -q_1 q_2^2 q_3^2 q_4 C_1 C_3^2 C_4 S_2^2 \gamma_1\gamma_2\gamma_3 z^{-(M+N+O)} \quad (7.d)$$

$$T_{5,1}^3(z) = -q_1 q_2^2 q_3^3 q_4 C_1 C_2^2 C_4 S_3^2 \gamma_1\gamma_2\gamma_3 z^{-(M+N+O)} \quad (7.e)$$

$$T_{1,2,3}^3(z) = q_1 q_2^2 q_3^2 q_4 C_1 C_2^2 C_3^2 C_4 \gamma_1\gamma_2\gamma_3 z^{-(M+N+O)} \quad (7.f)$$

In conclusion, the overall transmittance $T_f(z)$ of the triple RR architecture shown in Fig. 2(b), has been calculated according to Eq. (4).

In the design of optical filters based on triple RRs, we have set the coefficient q_i always equal to 1. In addition, the average ring loss per unit length α_i has been set to 0.1 dB/cm, resulting in low amplitude attenuations of transmission peaks characterizing overall transmittances, with respect to the ideal condition (α_i = 0 dB/cm).

III. Design Procedure

The mathematical model presented in previous section, is a useful tool for designing optical filters. In fact, several parameters can be dynamically changed for parametric investigations, i.e., RR lengths L_i, directional coupler coefficients k_i, propagation losses α_i, effective index n_{eff}, coefficients M, N and O.

In this work, the aim is to design triple RR optical filters characterized by an overall transfer function with desired wide-FSR. Then, the relationship between FSRs of three different RRs in the cascaded architecture sketched in Fig. 2(a) and 2(b), is given by:

$$FSR_{TOT} = FSR_1 \cdot M = FSR_2 \cdot N = FSR_3 \cdot O \quad (8)$$

where FSR_i is the i^{th} RR free spectral range and FSR_{TOT} is the desired free spectral range to be set as design specification. Moreover, Eq. (8) imposes a direct relationship between the perimeter lengths L_i of each RR. This one can be derived by writing FSR_i according to Eq. (2), as follows:

$$FSR_{TOT} = \frac{M \cdot c}{L_1 \cdot n_{eff,1}} = \frac{N \cdot c}{L_2 \cdot n_{eff,2}} = \frac{O \cdot c}{L_3 \cdot n_{eff,3}} \quad (9)$$

In particular, by ideally considering the phase-matching in terms of propagation constants of waveguide modes, i.e., $\beta_1 = \beta_2 = \beta_3$, being β_i the propagation constant in the i^{th} RR, it results in: $n_{eff,1} = n_{eff,2} = n_{eff,3} = n_{eff,TE} = 3.323135$.

By considering T_1 as the reference delay, the relationship between single roundtrip delays T_i can be expressed as:

$$FSR_{TOT} = \frac{M}{T_1} = \frac{N}{T_2} = \frac{O}{T_3} \Rightarrow T_2 = \frac{N}{M} T_1, T_3 = \frac{O}{M} T_1 \quad (10)$$

All roundtrip delays occur for the definition of the overall transmittance of the optical filter, through the frequency domain variable z, as in Eq. (6.a)-(6.f) and Eq. (7.a)-(7.f). In particular, the following equations are obtained:

$$z^{-M} = \exp(-j2\pi\nu T_1) \quad (11.a)$$

$$z^{-N} = \exp(-j2\pi\nu T_1 \frac{N}{M}) \quad (11.b)$$

$$z^{-O} = \exp(-j2\pi\nu T_1 \frac{O}{M}) \quad (11.c)$$

$$z^{-(M+N)} = \exp(-j2\pi\nu T_1[1+\frac{N}{M}]) \quad (11.d)$$

$$z^{-(N+O)} = \exp(-j2\pi\nu T_1[\frac{N+O}{M}]) \quad (11.e)$$

$$z^{-(M+O)} = \exp(-j2\pi\nu T_1[1+\frac{O}{M}]) \quad (11.f)$$

$$z^{-(M+N+O)} = \exp(-j2\pi\nu T_1[\frac{M+N+O}{M}]) \quad (11.g)$$

A. Coefficient Map

The mathematical analysis evidences how FSR_{TOT} mainly depends on geometrical and optical properties of the cascaded architecture, working as an optical filter.

In this context, a coefficient map has been realized as a bi-dimensional space in which coefficients M, N and O and ratios N/M and O/M are plotted as a function of FSRTOT. The importance of monitoring these coefficients and their relative ratios is clear from Eq. (10).

The design procedure starts by defining the perimeter length of the longest RR, i.e., the first one from the top of the cascaded architecture in Fig. 2. Consequently, perimeter lengths of remaining RRs are automatically calculated according to Eq. (9), in case of phase-matching condition:

$$L_2 = L_1 \cdot \frac{N}{M}, L_3 = L_1 \cdot \frac{O}{M} \quad (12)$$

The initial set of coefficients is always identified by the combination M = 3, N = 2 and O = 1, representing the lowest available set of different natural and co-prime numbers. In particular, the trivial combination identified by $M = N = O = 1$ is acceptable but intentionally not considered because it corresponds to identical RR perimeter lengths, as it is possible to verify from Eq. (12).

An example of design procedure is presented in this section for triple RR filter design with FSR_{TOT} = 12 THz. The procedure starts by setting L_1 = 104.595 μm. Consequently, perimeter lengths and FSRs are listed in Table 1, with FSR_{TOT} = 2.587 THz (i.e., 20.732 nm).

TABLE 1: RR GEOMETRICAL PARAMETERS AND FSRS.

	L (μm)	*R (μm)*	*FSR (THz)*
Ring 1	104.59	16.65	0.863
Ring 2	69.73	11.1	1.294
Ring 3	34.86	5.55	2.587

The coefficient map for this cascaded architecture is plotted in Fig. 3.

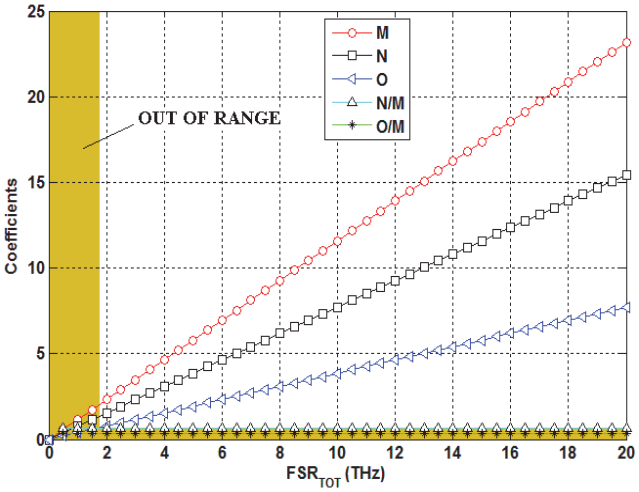

Fig. 3. Coefficient map of triple RR optical filter. Parameters: L_1 = 104.59 μm, M = 3, N = 2 and O = 1.

Combinations of coefficients M, N and O and corresponding FSR_{TOT}, cannot be chosen in the region labeled as "out of range", because relationships between FSRs, as in Eq. (8), do not hold for the specific architecture. In particular, the "out of range" domain is generated when one or both constant ratios N/M and O/M intersect at least one of the linear functions associated to coefficients M, N and O. In fact, at these intersection points one or more of these expressions must hold:

$$\frac{N}{M}=M;\frac{N}{M}=N;\frac{N}{M}=O;\frac{O}{M}=M;\frac{O}{M}=N;\frac{O}{M}=O. \quad (13)$$

which are impossible to be verified if coefficients M, N and O are natural and co-prime numbers, as required by the model.

Once selected FSR_{TOT} in the coefficient map, the corresponding set of coefficients is generally characterized by fixed-point numbers. Consequently, M, N, and O have to be usually approximated to the nearest integers (indicated with variables M^{int}, N^{int} and O^{int}, respectively). In addition, it is possible that for a given FSR_{TOT}, the corresponding coefficients are not co-prime. In this case, since an approximation cannot be found for the selected architecture, then possible solutions consist in changing the initial value of L_1 or choosing a different FSR_{TOT}.

In the design of the optical filter characterized by FSR_{TOT} = 12 THz, it is needed to use the coefficient map in Fig. 3 for estimating a novel coefficient set of RR perimeter lengths, able to satisfy the requirement. Numerical results are listed in Table 2.

TABLE 2: COEFFICIENTS SELECTED FOR FSR_{TOT} = 12 THZ.

Coefficients	*Initial set*	*Final set*
M	-	13.91
M^{int}	3	14
N	-	9.27
N^{int}	2	9
O	-	4.63
O^{int}	1	5
FSR_{TOT} (THz)	2.587	12.1

A useful comparison between overall transmittances exhibited by triple RR architectures, designed with initial and final sets of coefficients, is plotted in Fig. 4.

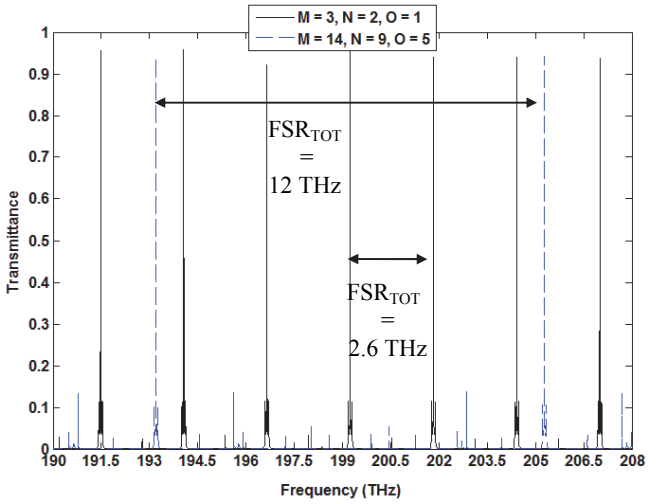

Fig. 4. Overall transmittances calculated with initial and final set of coefficients, corresponding to FSR_{TOT} = 2.6 THz and FSR_{TOT} = 12 THz, respectively.

The approximation introduced by considering the nearest integers of the selected coefficients, causes a numerical discrepancy between desired and calculated FSR. In particular, the larger the approximation of selected coefficients (e.g., $|M-M^{int}|$), the larger the error introduced in the calculated FSRs. Consequently, the choice of coefficients M, N and O represents an important design step, since the difference between the coefficients selected from the map (see Fig. 3) and their nearest integers is to be minimized.

The set of approximated coefficients allows upgrading the RR perimeter lengths for optical filter fabrication, as listed in Table 3 below. In particular, it is possible to calculate new values of L_2 and L_3 by using Eq. (12).

TABLE 3: RR GEOMETRICAL PARAMETERS AND FSRS.

	L (μm)	*R (μm)*	*FSR (THz)*
Ring 1	104.59	16.646	0.863
Ring 2	67.24	10.701	1.342
Ring 3	37.36	5.945	2.415

By comparing Tables 1 and 3, it is evident that micrometer variations of RR perimeter lengths should induce the suppression of several resonances in the overall

transmittance, producing a desired FSR_{TOT}. Obviously, if the initial coefficient combination is set to $M = N = O = 1$, linear functions in the coefficient map are overlapped for every value of FSR_{TOT} because of the same function slope, making it impossible to design the optical filter with desired FSR.

Although different and arbitrary values of RR perimeter length L_1 can be selected at the beginning of the design procedure, small values of L_1 can still cause some problems. For example, by selecting L_1 = 50 µm, the remaining RR perimeter lengths are L_2 = 33.33 µm and L_3 = 16.67 µm resulting in very small RR radii, i.e., R_2 = 5.3 µm and R_3 = 2.65 µm, respectively. Obviously, the radius R_3 is really too small and should surely induce high radiation losses, so degrading the filter performance.

In addition, by reducing RR perimeter lengths, the bi-dimensional space associated to the coefficient map should be minimized, resulting in a limited set of available FSR_{TOT} values. In Fig. 5 it is possible to observe different linear functions of the coefficient M calculated as a function of decreasing perimeter lengths L_1.

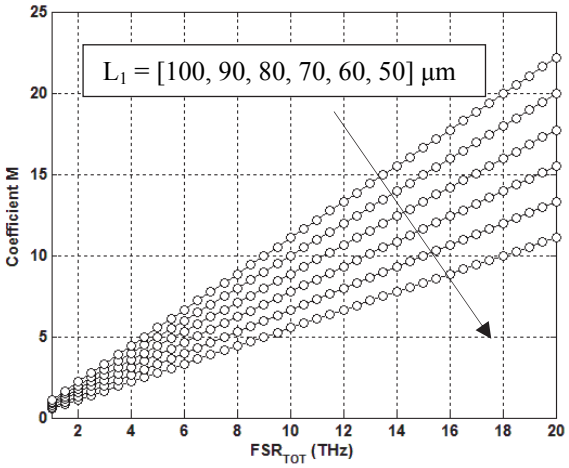

Fig. 5. Linear function of coefficient M as a function of FSR_{TOT} and decreasing perimeter lengths L_1.

Similar trends also characterize the linear functions associated to coefficients N and O. Consequently, by reducing the geometrical dimensions of the cascaded architecture, the "out of range" region will represent a great percentage of the bi-dimensional space, resulting in a wrong design procedure.

The utility of the coefficient map can be appreciated by monitoring the changes of FSR_{TOT} generated in two different design approaches. In the first one, the cascaded architecture designed with coefficients M = 14, N = 9, O = 5, and characterized by geometrical parameters as listed in Table 3, is simulated as a function of increasing values of L_1, with the same coefficient set as before. In the second approach, for each value of L_1 a new set of coefficients is derived from the corresponding coefficient map, in order to obtain the target FSR_{TOT} = 12 THz. Numerical results are shown in Fig. 6.

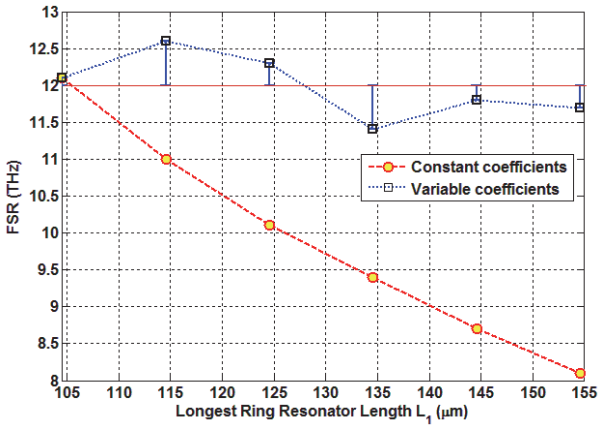

Fig. 6. FSRs of overall transmittances calculated with constant and variable coefficient sets.

In the first approach, FSR_{TOT} of overall transmittance decreases with increasing L_1, so giving a wrong design procedure, not able to satisfy the design specification. In the second one, the coefficient map has been upgraded for each value of L_1 and a new set of coefficients (i.e., RR perimeter lengths) has been considered in order to hold the specification over FSR_{TOT}. Thus, a small ripple is revealed in Fig. 6, due to the approximation introduced by considering integer values of coefficients M, N and O. In addition, for RR perimeter lengths L_1 = 114.6 µm, L_2 = 134.6 µm and L_1 = 154.6 µm, coefficients derived from the coefficient map are not co-prime (e.g., M = 15.24, N = 10.16, O = 5.081, M^{int} = 15, N^{int} = 10, O^{int} = 5 for L_1 = 114.6 µm), thus other sets have been chosen corresponding to the closest FSR_{TOT} values (e.g., 12.5 THz or 11.5 THz).

In conclusion, the coefficient map represents an important tool needed to set precise geometrical parameters (i.e., RR radii) of the triple RR optical filter for exhibiting the desired FSR_{TOT}.

B. Optimization of Power Coupling Ratio and Crosstalk

The design procedure described until now is finalized to the optimization of power coupling ratios k_1, k_2, k_3 and k_4, shown in schematized SFG of Fig. 2(a). To this purpose, we have verified that the optimal set of power coupling ratios is $k_1 = k_2 = 0.1$ and $k_3 = k_4 = 0.0025$ [16].

In particular, it is possible to analyze in Fig. 7 the effect of optimized and not-optimized power coupling ratios on the overall transmittance of the designed optical filter, windowed around a single transmission peak.

Thus, the coefficient sets $k_1 = k_2 = 0.38$, $k_3 = k_4 = 0.065$ and $k_1 = k_2 = 0.15$, $k_3 = k_4 = 0.065$ are not acceptable because of the presence of high secondary transmission peaks, symmetrically disposed around the resonance frequency (i.e., 193.2 THz). The optimal coefficient set (i.e., $k_1 = k_2 = 0.1$, $k_3 = k_4 = 0.0025$) significantly reduces the amplitude of sidelobe transmission peaks, resulting in a very thin linewidth at 193.2 THz, so assuring a much better selectivity. Analogous features characterize other transmittance peaks, periodically spaced by 12 THz.

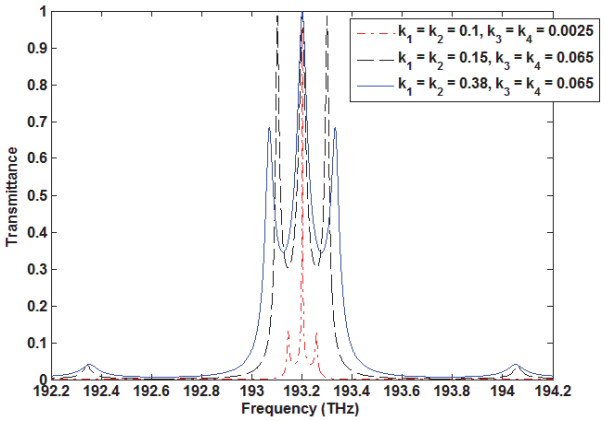

Fig. 7. Different overall transfer functions of designed optical filter (FSR_{TOT} = 12 THz) as a function of different sets of power coupling ratios.

In conclusion, it is possible to note in Table 4 the crosstalk variation as a function of FSR_{TOT} exhibited by triple RR optical filters, as designed with optimized power coupling ratios and suitable coefficients *M*, *N* and *O*.

TABLE 4: CROSSTALK AS A FUNCTION OF FSRS.

FSR_{TOT} (THz)	Crosstalk (dB)
10	-20.4164
12	-16.5596
17	-11.6772
19	-9.468

As demonstrated in Ref. [16], the closer the FSR of the overall transmittance, the lower the crosstalk of resulting optical filter.

IV. CONCLUSION

In this paper the modeling and design of an optical filter based on a triple RR cascaded architecture operating in C and L bands is proposed. The developed general procedure of design allows interesting performances in terms of wide FSR as large as 100 nm, high selectivity and low crosstalk (-20 dB), to be achieved. The proposed model allows customizing the design of integrated and high-performance CMOS-compatible OADMs and ROADMs [16]. The cascaded architecture is also suitable for fabrication of modular router configurations, such as those based on the Manhattan layout, for applications in high speed ultra DWDM on-chip optical interconnects. Further investigations should be dedicated to rigorous treatment of higher order effects, including dispersion of absorption coefficients and phase-mismatching. However, the influence of these effects is usually small and also negligible due to the intrinsic feature of the proposed design method, i.e., the approximation of coefficients to their nearest integers.

REFERENCES

[1] B. Mikkelsen, G. Raybon, R. -J. Essiambre, A. J. Stenz, T. N. Nielsen, D. W. Peckham, L. Hsu, L. Gruner-Nielsen, K. Dreyer, and J. E. Johnson, "320-Gb/s single channel pseudo-linear transmission over 200 km of nonzero-dispersion", *IEEE Photon. Technol. Lett.*, Vol. 12, No. 10, pp. 1400-1402 (2000).

[2] M. Irfan Anis, K. Zaka, N. Ahmed, and U. Ahmed, "Performance analysis of optical network based on OADM by using different filters", *AH-ICI 2009*, pp. 1-5, (2009), ISBN: 978-1-4244-4569-1.

[3] P. Dong, N-N Feng, D. Feng, W. Qian, H. Liang, D. C. Lee, B. J. Luff, M. Asghari, A. Agarwal, T. Banwell, R. Menendez, P. Toliver, and T. K. Woodward, "A Tunable Optical Channelizing Filter Using Silicon Coupled Ring Resonator", *CLEO-QELS 2010 Conf.*, pp. 1-2 (2010).

[4] M. Mancinelli, R. Guider, P. Bettotti, M. Masi, M.R. Vanacharla, and L. Pavesi, "Coupled-resonator-induced-transparency, concept for wavelength routing applications", *Opt. Express*, Vol. 19, No. 13, pp. 12227-12240 (2011).

[5] E. J. Klein, D. H. Geuzebroek, H. Kelderman, and A. Driessen, "Integrated optical add-drop multiplexer using thermally tunable microring resonators", *IEEE/LEOS Benelux Chapter 2004 Annual Symposium*, pp. 103-106 (2004), ISBN: 978-9-0765-4606-3.

[6] M. Geng, L. Jia, L. Zhang, L. Yang, P. Chen, T. Wang, and Y. Liu, "Four-channel reconfigurable optical add-drop multiplexer based on photonic wire waveguide", *Opt. Express*, Vol. 17, No. 7, pp. 5502-5516 (2009).

[7] M. A. Popovic, T. Barwicz, M. S. Dahlem, F. Gan, C. W. Holzwarth, P. T. Rakich, H. I. Smith, E. P. Ippen and F. X. Kartner, "Tunable, Fourth-Order Silicon Microring-Resonator Add-Drop Filters", *33rd ECOC*, pp. 1-2 (2007), ISBN: 978-3-8007-3042-1.

[8] A. M. Prabhu, Z. Han, A. Tsay, and V. Van, "Wideband 1.5µm-radius SOI add-drop microring filter for WDM on chip interconnects", *CLEO-QELS 2009 Conf.*, pp. 1-2 (2009).

[9] J. Garcia, A. Martinez, and J. Marti, "Optical Add-Drop Multiplexer with FSR Higher than 140 nm using Ring Resonators and Photonic Bandgap Structures", *5th IEEE GFP Conf.*, pp. 82-84 (2008).

[10] Z. Qiang, W. Zhou, and R. A. Soref, "Optical add-drop filters based on photonic crystal ring resonators", *Opt. Express*, Vol. 15., No. 14, pp. 1823-1832 (2007).

[11] J. Feng, Q. Li and Z. Zhou, "Single Ring Interferometer Configuration With Doubled Free-Spectral Range", *IEEE Photon. Technol. Lett.*, Vol. 23, No. 2, pp. 79-81 (2011).

[12] R. Grover, V. Van, T. A. Ibrahim, P. P. Absil, L. C. Calhoun, F. G. Johnson, J. V. Hryniewicz, and P.-T. Ho, "Parallel-Cascaded Semiconductor Microring Resonators for High-Order and Wide-FSR Filters", *J. Lightwave Technol.*, Vol. 20, No. 5, pp. 900-905 (2002).

[13] Y. Yanagase, S. Suzuki, Y. Kokubun, and S. T. Chu, "Box-Like Filter Response and Expansion of FSR by a Vertically Triple Coupled Microring Resonator Filter". *J. Lightwave Technol.*, Vol. 20, No. 8, pp. 1525-1529 (2009).

[14] Comsol Multiphysics by COMSOL ©, ver 3.2, single license (2005).

[15] S. Mandal, K. Dasgupta, T. K. Basak, and S. K. Ghosh, "A generalized approach for modeling and analysis of ring-resonator performance as optical filter", *Opt. Commun.*, Vol. 264, No. 1, pp. 97-104, (2006).

[16] B. Troia, V. M. N. Passaro, andF. De Leonardis, "Design of Optical Filters Based on Multiple Ring Resonators Operating in C and L Bands", *Conf. Proc. of the 19th Telecommun. Forum (TELFOR 2011)*, pp. 820-823 (2011), ISBN: 978-1-4577-1498-6.